Eur. Phys. J. B **39**, 397–408 (2004)
DOI: 10.1140/epjb/e2004-00205-y

THE EUROPEAN PHYSICAL JOURNAL B

Many-neighbour interaction and non-locality in traffic models

R.E. Wilson[1,a], P. Berg[2,b], S. Hooper[1], and G. Lunt[3]

[1] Department of Engineering Mathematics, University of Bristol, University Walk, Bristol BS8 1TR, UK
[2] School of Science, UOIT, 2000 Simcoe St North, Oshawa, ON, L1H 7L7, Canada
[3] TRL Ltd., Old Wokingham Road, Crowthorne, RG45 6AU, UK

Received 3rd December 2003 / Received in final form 27 March 2004
Published online 12 July 2004 –

Abstract. The optimal-velocity model, as proposed by Bando et al. [1], shows unrealistic values of the acceleration for various optimal-velocity functions [2,3]. We discuss different approaches of how to correct this problem. Multiple look-ahead (many-neighbour interaction) models are the most promising candidates in reducing accelerations and decelerations to realistic values. We focus on two such models and, in particular, their linear stability and how these affect the vehicle dynamics and wave solutions. As found earlier [4], multiple look-ahead models reproduce many real flow features, and our results further support the necessity of this ansatz. However, the problem of non-locality arises when they are transformed into the corresponding continuum model. We discuss three methods of how to interpret many-neighbour interaction in macroscopic models.

PACS. 45.70.Vn Granular models of complex systems; traffic flow – 89.90.+n Other topics in areas of applied and interdisciplinary physics – 47.50.+d Non-Newtonian fluid flows

1 Introduction

Highway traffic has been a growing area of research for almost fifty years [5–7]. As our roads become more congested, this research will take on a greater significance to modern society. It is therefore important to develop a basic understanding of how traffic behaves in order to adapt our road networks to best serve driver needs.

This publication is concerned with the optimal-velocity (OV) model proposed by Bando et al. [1] and some modifications to it, which are aimed at adding extra realism to the solutions. The original (standard OV) model, which has attracted much interest in the traffic modelling community, contains some unrealistic features such as crashes (Sect. 2.1) and extreme values for both the acceleration and deceleration (Sect. 2.2).

Based on numerical simulations, we will discuss explicit limitations of acceleration and deceleration (Sect. 3), time delay (Sect. 4) and multiple look-ahead (Sects. 5 and 7) as candidates for achieving such goals. For the latter case, we also present a stability analysis (Sect. 6). We conclude with an analysis of modelling multiple look-ahead in continuum models in Section 8, where the problem of non-locality arises.

We would like to mention at this point that this project was supported by TRL Ltd who have, as one of their major activities, the development of simulation software to model real life motorway scenarios.

[a] e-mail: re.wilson@bristol.ac.uk
[b] e-mail: peterberg@pims.math.ca

2 The optimal-velocity model: set-backs and modifications

In the optimal-velocity car-following model of Bando et al. [1], the acceleration of every car is determined by its velocity v_n and a desired speed $V_n(b_n)$ depending on the *headway* b_n to the car in front

$$\dot{v_n} = a_n \left[V_n(b_n) - v_n \right]. \tag{1}$$

Here, $V_n(b_n)$ is called the optimal-velocity (OV) function and a_n the driver's sensitivity. The headway b_n is the distance of the nth car to the car ahead

$$b_n(t) = x_{n-1}(t) - x_n(t) \tag{2}$$

with

$$\dot{x}_n(t) = v_n(t). \tag{3}$$

As mentioned earlier, this model is able to reproduce various features of road traffic and has been the subject of much research [8–10]. In what follows, we will adopt the usual approach of setting all OV functions and sensitivities to be the same, $V_n \equiv V$ and $a_n \equiv a$, respectively. This corresponds effectively to modelling single-species traffic [11]. In addition and unless stated otherwise, we

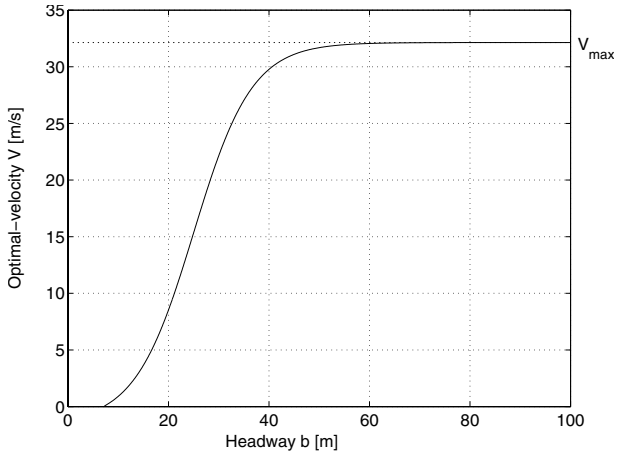

Fig. 1. The optimal-velocity function of Bando et al. [2], equation (4). Maximum gradient and turning point at $b = 25$ m.

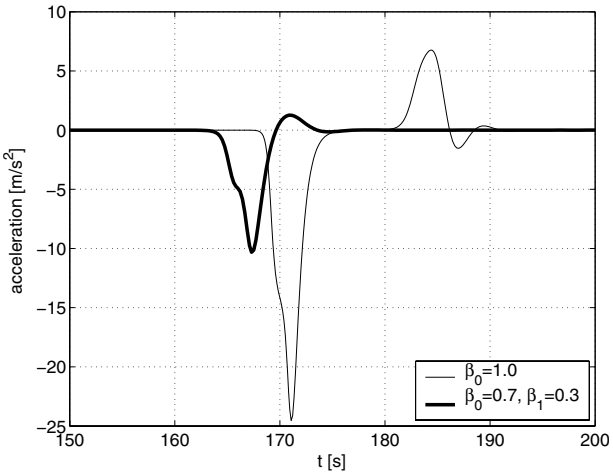

Fig. 2. Plot of acceleration of braking vehicle going through a travelling wave connecting upstream headways, $b_u = 60$ m, with downstream headways, $b_d = 20$ m, in the OV model with OV function (4). Here, $a = 2.0\ \mathrm{s}^{-1}$. The unrealistic magnitudes in the simple look-ahead ($\beta_0 = 1.0$) model can be reduced drastically to more reasonable values by double look-ahead, $\beta_0 = 0.7$, $\beta_1 = 0.3$ (see Sect. 5 for definition of $\{\beta_i\}$).

choose $a = 2.0\ \mathrm{s}^{-1}$ and the OV function proposed by Bando et al. [9]

$$V(b) = \max\{0, 16.8\,[\tanh(0.0860(b-25)) + 0.913]\}\ \mathrm{m/s}, \tag{4}$$

based on real traffic data gathered from Japanese motorways, as shown in Figure 1.

2.1 Crashes

Despite being one of the most promising candidates among all car-following models, the OV model has major setbacks. We found the occurrence of crashes at values of the sensitivity smaller than about one, $a \leq 1\ \mathrm{s}^{-1}$. Such incidents take place on a circular road, for example, as the shock waves of stop-and-go traffic steepen until vehicle trajectories finally overlap.

One might argue that such behaviour might be avoided by simply taking values $1\ \mathrm{s}^{-1} < a < 2\ \mathrm{s}^{-1}$ so that crashes will not occur, but stop-and-go traffic still evolves. However, small values of the sensitivity are typical for vehicles of large inertia [12], and we will see in the next section that this issue cannot be tackled quite that simply. The root of the problem lies in unrealistic acceleration.

2.2 Acceleration and breaking

Although stability is strongly dependent on the shape of the OV function (Sect. 6), we find that when using one that is calibrated from real traffic data such as in equation (4), a major problem arises in the maximum values of the acceleration and deceleration [3,9]. Arguably, this represents the biggest set-back of the standard OV model.

As an example, we investigated the acceleration of one vehicle on a straight road (Fig. 2), going through a travelling wave pattern connecting two different headways.

We observed absolute values of acceleration up to 25 $\mathrm{m/s}^2$, substantially above any realistic value. In fact, we were not able to determine an OV function which gives reasonable values for the acceleration and the right orders for the speed-headway relation, while at the same time reproducing a sensible fundamental diagram including a region of instability close to real data. This raises the question as to what extent the standard model represents real traffic flow. As presented in what follows, one might be tempted to deal with this problem in three different ways:

1. limiting the acceleration/deceleration explicitly;
2. introduce delay;
3. introduce multiple look-ahead (many-neighbour interaction) coupling a car to more than one vehicle ahead.

Before we continue it shall be pointed out, though, that Gipps [13] developed a model which incorporated a maximum and minimum acceleration that a driver would wish to undertake. These values took mean values of 1.7 $\mathrm{m/s}^2$ and $-3.4\mathrm{m/s}^2$, respectively. This model is widely used in engineering circles to simulate traffic flow, and the values were taken from experiments with real traffic.

In addition, Sugiyama et al. [14] and Wagner et al. [15] have carried out extensive fitting of models to vehicle data based on minimising discrepancies of headway and velocity between data and model predictions. Acceleration, however, did not play a role in the fitting routines so that this unrealistic model feature was not further investigated.

3 Limiting the acceleration and breaking of vehicles by cut-off

In the previous section, we saw that when uniform flow is stable and crashes do not occur, travelling waves may form in which individual vehicles may have unrealistic accelerations. In this section, we attempt to remedy this

problem by replacing the linear velocity-difference acceleration law in equation (1) with a nonlinear (non-smooth) acceleration law. (Note that the standard OV model is already most generally nonlinear as the OV function may be nonlinear.)

Our modified model is

$$\ddot{x}_n = \mathrm{mid}\left\{-a_{\min}, a\left[V(b_n) - \dot{x}_n\right], a_{\max}\right\}, \qquad (5)$$

where $a_{\min}, a_{\max} > 0$. This model states that if the difference of optimal velocity and actual velocity is small, then acceleration is given by the usual linear-in-velocity difference law. If the velocity difference is larger, so that the standard model would produce a large acceleration, then a saturated maximum acceleration $a_{\max}$ or maximum breaking $a_{\min}$ is produced.

The standard OV model is equivalent to equation (5) with $a_{\min}, a_{\max} \to \infty$. To simplify matters, we briefly consider the cases of "limiting breaking and acceleration" ($a_{\min}$ finite, $a_{\max}$ finite), "limiting only acceleration" ($a_{\min}$ infinite, $a_{\max}$ finite), and "limiting only breaking" ($a_{\min}$ finite, $a_{\max}$ infinite).

Note that the linear stability of the uniform flow solutions of equation (5) is identical to that of the standard OV model (Sect. 6), as small perturbations to uniform flow are unchanged in this modified equation. However, the global solution behaviour may be different.

3.1 Restrict maximum and minimum acceleration

Restricting both the maximum and minimum accelerations to 13 m/s^2, we found that shock waves are travelling at a slower speed upstream than previously observed. Moreover, reducing the accelerations to 12 m/s^2 produced crashes. This is not desirable as we are trying to produce realistic accelerations and driver behaviour.

We conclude that restricting maximum and minimum acceleration at the same time by a cut-off leads to crashes and, hence, an unrealistic traffic flow model.

3.2 Restrict positive acceleration

First, we allow unlimited breaking and restrict the positive acceleration of vehicles. In this regime, one would think that crashes do not occur, as drivers may brake as hard as they desire. This is usually true. When the maximum acceleration is limited to 10 m/s^2 and 1.7 m/s^2, respectively (the latter is the value given by Gipps [13] as the maximum desired acceleration that a driver would want to undertake), the maximum breaking undertaken by drivers increases to -19.81 m/s^2 and -23.11 m/s^2, respectively. This means that there are even more unrealistic accelerations than before. Also by reducing $a_{\max}$, the severity of shock waves is generally increased.

We conclude that this method also fails to produce more realistic values for the acceleration of vehicles in a platoon.

3.3 Restrict breaking

Conversely, when restricting the breaking capability of vehicles but allowing positive acceleration to be unlimited, one would expect problems to occur, as vehicles would not be able to slow down quickly enough when they approach the congested region. Limiting breaking to 5 m/s^2 causes crashes and the maximum acceleration that is achieved is 21.98 m/s^2. Note that the maximum theoretical value of acceleration is $\dot{v}_{\max} = aV(b \to \infty) = 32.14a$ m/s. However, the latter value of 21.98 m/s^2 does not have any real significance as the model brakes down after the first crash. In any case, the values of acceleration are wholly unrealistic, and the method fails.

In the context of realistic accelerations, the question is raised as to which values of the sensitivity, a, have physical meaning for the OV model. Without pilot vehicle data — that is data gathered by tracking an individual vehicle as it moves through traffic and monitoring its behaviour — it is not possible to fit a (in contrast to the speed-headway function which can be fitted from (MIDAS) data loops, for example; see Abou-Rahme [16]). One way to determine a minimum value of a is to investigate the issue of whether a car starting from infinity is able to come to rest safely behind a stationary object [3], modelled by the standard OV model.

To conclude this chapter, it appears that our intuitive idea for limiting the magnitude of acceleration is not successful. Accelerations and decelerations may not be strongly limited together without causing vehicles to crash. It is possible to limit only accelerations without causing crashes, but then the values of deceleration produced are even more unrealistic than before. Similar conclusion hold in the opposite case of limiting breaking only.

4 Time delay

Another drawback to the standard OV model is that it does not account for the reaction time of drivers. It assumes that the driver of a vehicle can instantaneously decide and act on what is happening around him. This is obviously not the case in real life. Drivers need time to size up the actions around them, weigh up the options and then act. Thus in this section, we look at adding in a delay to the standard OV model to represent drivers' reaction time and investigate in how far this affects the maximum values of acceleration and deceleration in the system.

We follow the delay model of Bando et al. [9]

$$\dot{v_n}(t+T) = a\left[V(b_n(t)) - v_n(t)\right] \qquad (6)$$

with an explicit delay time T. There has been previous work on this model [9,17], in which linear stability analysis and numerical simulations were carried out.

Bando et al. [9] argue that there exist two regimes for the delay time. For $T < 0.2$ s, the delay does not have much of an effect on the flow solution and can be disregarded. For $T > 0.2$ s, it has a very remarkable effect on

the flow leading to unphysical flow solutions. The authors conclude that an upper bound for the delay time has to be introduced to avoid such scenarios.

Davis [17], however, argues that this is actually a setback of the OV model in that it does not allow for realistic explicit delay times of the order of 1 second [18]. In this case, the author has observed the occurrence of crashes which should not occur in the model for the parameters used in his study.

In addition to confirming his results, we have found that keeping a fixed at $a = 3.0\ \mathrm{s}^{-1}$ and increasing T from 0.25 s to 0.3 s results in unrealistic backwards moving vehicles. This is in full agreement with the observation by Bando et al. [9]. However, we interpret this occurrence of backwards moving vehicles without crashes as a failure of the model rather than limiting T to values smaller than 0.2 s [18].

Moreover, we found that the recommended restriction to $T < 0.2$ s does not solve the problem of unrealistic acceleration and breaking, and has only a miniscule impact. Since this is what we were trying to solve with the explicit introduction of delay, we conclude that delay time (alone) does not resolve in a realistic OV traffic flow model.

The same conclusion holds true for other delay models. One example is a model suggested by Nagatani et al. [19] which extends the OV model (1–3) by an ODE for the relaxation of the optimal velocity, V_n, itself

$$\dot{V}_n = b\left\{aV(b_n) - V_n\right\}. \tag{7}$$

Here, the additional variable V_n replaces $V_n(b_n)$ in (1), and $V(b_n)$ is some optimal-velocity function. This model, which is strictly speaking not a delay but a relaxation model, has very interesting features with respect to metastability and flow transitions but cannot solve the problem of large accelerations.

5 Multiple look-ahead in optimal-velocity models

In this section, we perform our final modification to the OV model. We introduce terms to model the anticipation of drivers, who in reality act not only to the behaviour of the vehicle directly in front, but also to the behaviour of those further ahead. We analyse two different interpretations of this idea, which we refer to as model A and model B.

5.1 Model A

We consider

$$\dot{v}_n = a\left\{\sum_{j=0}^{k}\beta_j V(b_{n-j}) - v_n\right\}, \tag{8}$$

where $\beta_j > 0$ and $\sum_{j=0}^{k}\beta_j = 1$ so that uniform flow solutions are the same as in the standard OV model ($k = 0$). Here, the optimal velocity of a driver is given by a weighted sum of the speed-headway function evaluated at his/her own headway and at the headways of several vehicles in front. Thus, if the headway of vehicle $n-1$ is small, then vehicle n will have a lower optimal velocity than in the standard OV model. Hence, vehicle n will tend to brake earlier when approaching congested traffic.

A model which somewhat falls into this category was proposed by Nagatani [20] in the form of a difference equation modelling time delay τ. The coupling to two vehicles ahead is described by

$$x_n(t+2\tau) = x_n(t+\tau) + \tau\left[(1-\beta)V(b_n(t)) + \beta V(b_{n-1}(t))\right]. \tag{9}$$

Difference equations are beyond the scope of this paper (see also the Kerner-Klenov model [21]). However, it should be noted that the author observed less severe accelerations and an overall stabilisation of the flow in the numerical simulations (see also Sect. 7).

One would expect the β_j to decrease as j increases, as drivers would tend to weight the headway of vehicles closer to them more importantly than those further ahead. However, they might generally depend on time.

5.2 Model B

This model is taken from Lenz et al. [4,22]. We suppose that the optimal velocity of driver n is given by a weighted sum of the original OV function, evaluated at the distance (suitably normalised) to each of several vehicles ahead. We have

$$\dot{v}_n = a\left\{\sum_{j=0}^{k}\beta_j V\left(\frac{\sum_{l=0}^{j} b_{n-l}}{j+1}\right) - v_n\right\} \tag{10}$$

where again $\beta_j > 0$ and $\sum_{j=0}^{k}\beta_j = 1$ so that uniform flow solutions are the same as in the standard OV model.

Arguably, model A seems more intuitive, since the driver anticipates likely reactions of further drivers ahead, more so than a driver in model B. However, Lenz et al. have found model B to reveal some very interesting features, some of which can be validated against real traffic data such as the speed of shocks in stop-and-go traffic.

5.3 Other models

There are many more ways to define multiple look-ahead models based on the standard OV model. An example is

$$\dot{v}_n = a\left\{V\left(\sum_{j=0}^{k}\beta_j b_{n-j}\right) - v_n\right\}, \tag{11}$$

corresponding to the standard OV model with an average (weighted) headway, $\sum_{j=0}^{k}\beta_j b_{n-j}$, and $\sum_{j=0}^{k}\beta_j = 1$. However, we will not further pursue other models but

should be aware of the fact that there is no unique modelling of many-neighbour interaction.

In what follows, we refer to *single look-ahead* or *simple look-ahead* when $\beta_0 = 1.0$ and $\beta_j = 0$ for $j > 1$. Correspondingly, we define *double look-ahead* as β_0, $\beta_1 \neq 0$ and $\beta_j = 0$ for $j > 1$, and *triple look-ahead* as β_0, β_1, $\beta_2 \neq 0$ and $\beta_j = 0$ for $j > 2$.

6 Stability analysis

6.1 Standard OV model

The standard OV model, equation (1), is unstable towards arbitrarily small perturbations of uniform flow solutions when

$$2V'(b) > a \tag{12}$$

holds [2]. This defines a critical sensitivity a_{crit}, above which the flow is always linearly stable, depending on the chosen OV function. For values of a smaller than a_{crit}, this defines also an intermediate density regime where the flow is linearly unstable [2], which is in accordance with traffic data. This (and the meta-stable regime [23]) is where stop-and-go traffic patterns emerge from [2,24]. Hence, any modified OV model must still reproduce a linearly unstable density regime or it should otherwise be disregarded.

6.2 Model A

We will now investigate how the instability is affected by the inclusion of multiple look-ahead terms.

Following the analysis of Appendix A, the neutral stability line in the a–b plane is defined by

$$\frac{V'(b)}{a} = -\frac{\sum_{j=0}^{k} \beta_j \left\{\cos[(j+1)\xi] - \cos(j\xi)\right\}}{\left\{\sum_{j=0}^{k} \beta_j \left\{\sin[(j+1)\xi] - \sin(j\xi)\right\}\right\}^2}, \tag{13}$$

where we assume perturbations of the nth vehicle to the uniform flow solution proportional to $e^{\lambda t}\, e^{in\xi}$.

This equation is still rather complicated in its full generality, so we analyse it by considering some special cases.

6.2.1 All β_i equal

If $\beta_j \equiv \beta = 1/(k+1)$, neutral stability is now defined by (see Appendix A)

$$\frac{V'(b)}{a} = \frac{k+1}{2}. \tag{14}$$

Notice that for $k = 0$, i.e. the standard OV model, the stability criterion checks with that which was obtained in the previous section, equation (12).

We observe from equation (14) that when k is increased, the flow tends to be more stable, i.e. for the same V and b, a must be smaller for unstable flow. This is in accordance with results found in other many-neighbour interaction models (see Nagatani [20] and Sect. 6.2.4 [4]).

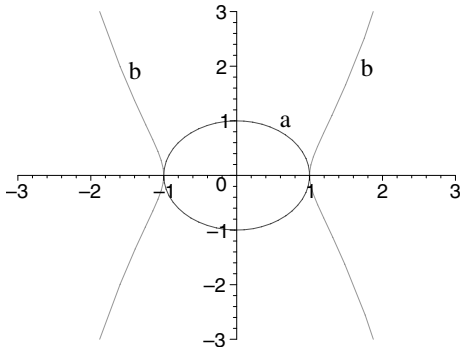

Fig. 3. Polar coordinates (angle ξ) plot of the linear stability criterion for double look-ahead, $\beta = (1/2, 1/2)$. b: right hand side of equation (46); a: left hand side of equation (46) set to be 1.0 where first instability occurs ($a = 1.44$ s^{-1}).

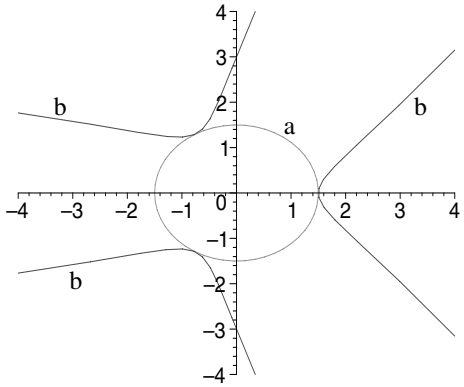

Fig. 4. Polar coordinates plot of the linear stability criterion for triple look-ahead, $\beta = (1/3, 1/3, 1/3)$. b: right hand side of equation (46); a: left hand side of equation (46) set to be 1.5 where first instability occurs ($a = 0.96$ s^{-1}).

For example, examine the case where $k = 1$ and $\beta = (1/2, 1/2)$. We wish to examine how instability occurs. This can be seen in Figure 3 where each side of equation (46) has been plotted separately using polar coordinates for $k = 1$. The left hand side is a circle taken to have radius 1 to illustrate the first time that the curves intersect, representing the onset of instability. Thus taking $b = 25$ m, so that $V'(b) = 1.44$ s^{-1}, solutions are stable for $a > 1.44$ s^{-1} and unstable for $a < 1.44$ s^{-1}, which is supported numerically with an initial value solver.

Similarly in Figure 4, the same curves have been plotted except now $k = 2$ and $\beta = (1/3, 1/3, 1/3)$. In this case, the singularities of the right hand side of equation (46) have the value $3/2$ at $\xi = 0, 2\pi/3$ and infinity at $\xi = \pi/3, \pi$. Here, the onset of instability is when the circle defined by the left hand side has value $3/2$. Thus taking $b = 25$ m, so that $V'(b) = 1.44$ s^{-1}, solutions are stable for $a > 0.96$ s^{-1} and unstable for $a < 0.96$ s^{-1}. Again, this is supported by numerical simulation.

$$2\frac{p'(\xi)}{q'(\xi)} = \frac{0.6\sin(3\xi) + 0.2\sin(2\xi) + 0.2\sin\xi}{[\{0.2\sin(3\xi) + 0.1\sin(2\xi) + 0.2\sin\xi\}\{0.6\cos(3\xi) + 0.2\cos(2\xi) + 0.2\cos\xi\}]}. \quad (16)$$

6.2.2 Take β_i different

Taking the β_j equal has only limited use, since they are generally going to decrease as j increases, because drivers attach less significance to the behaviour of vehicles far ahead. So we now consider the general case of different β_j.

It is not obvious where the potential singularities of the right hand side of equation (13) are, so we simplify by analysing a specific example. We choose $k = 2$ with $\beta_0 = 0.5$, $\beta_1 = 0.3$ and $\beta_2 = 0.2$. Then equation (13) becomes

$$\frac{V'(b)}{a} = -\frac{0.2\cos(3\xi) + 0.1\cos(2\xi) + 0.2\cos\xi - 0.5}{\{0.2\sin(3\xi) + 0.1\sin(2\xi) + 0.2\sin\xi\}^2}, \quad (15)$$

where we may denote the right hand side by $p(\xi)/q(\xi)$. This right hand side has potential singularities at $\xi = 0, \pi/2$ and π. (Again we consider only values of ξ between 0 and π, since the polar plot is symmetric in the horizontal axis.)

For $\xi = 0$ the numerator is also zero, and so we need further analysis to calculate the limit as $\xi \to 0$. Differentiating both top and bottom gives

see equation (16) above.

However at $\xi = 0$, both the numerator and denominator evaluate to zero. Thus we need to differentiate again and apply L'Hôpital and find

$$\lim_{\xi\to 0}\frac{p''(\xi)}{q''(\xi)} = 0.6. \quad (17)$$

However, for $\xi = \pi/2$ and π the numerator of equation (15) takes a negative value indicating that the right hand side tends to positive infinity at these values of ξ.

Figure 5 shows polar plots of the curves defined by each side of equation (15). The circle has radius $V'(b)/a = 1.2$, showing the first time the curves intersect. This again is where instability first occurs as a is decreased.

6.2.3 The $\xi = 0$ mode

Assuming that instability first occurs for long wave length perturbations (see Appendix A), we obtain the neutral stability criterion for general look-ahead

$$\frac{V'(b)}{a} = \frac{1}{2}\sum_{j=0}^{k}\beta_j(2j+1). \quad (18)$$

The standard OV model is retrieved at $k = 0$.

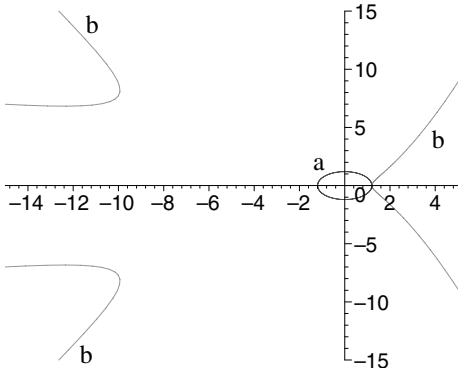

Fig. 5. Polar coordinates plot of the linear stability criterion for triple look-ahead, $\beta = (0.5, 0.3, 0.2)$. b: right hand side of equation (15); a: left hand side of equation (15) set to be 1.2 where first instability occurs.

6.2.4 Model B

The stability criterion for model B has been discussed in detail by Lenz et al. [4]. Without further reasoning, the authors also conclude that the first mode to go unstable occurs at $\xi = 0$. This is supported by the analysis of model A which shows this tendency in Figures 3, 4 and 5, reflected by equation (18). Now, we obtain neutral stability at $\xi = 0$ when

$$\frac{V'(b)}{a} = \frac{1}{2}\sum_{j=0}^{k}\beta_j(j+1). \quad (19)$$

As for model A, we find again that many-neighbour interaction leads to more stable flow. However, for the same initial uniform flow conditions (headway) and the same vector $\boldsymbol{\beta}$, model A is more stable than model B, meaning that a can be lower than in model B without reaching linear instability. This is somewhat reflected by the statement that one's reaction should also take into account the next likely reaction of the driver ahead.

We conclude that both model A and B leads to flows of higher stability than the standard OV model as they anticipate traffic events ahead. For model B, we refer for further analysis to Lenz et al. [4].

6.2.5 Maximum stability

It is easy to see that for $\beta_0 = 1$, the flow becomes more stable with the increase of any of the β_j $(j = 2, 3, ..., k)$. However, if we also impose

$$\sum_{j=0}^{k}\beta_j = 1 \quad (20)$$

and $\beta_j \geq 0$, there are one global maximum and minimum with respect to the overall linear stability of the flow: $\beta_k = 1$ and $\beta_0 = 1$, respectively. Upon maximising the functions given by the right hand sides of (18) and (19) subject to the condition (20) over the domain $0 \leq \beta_j \leq 1$ for $j = 1, ..., k$, a simple analysis with Lagrange multipliers reveals that there are no local extrema, but the global maximum and minimum stated above. In this sense, the standard optimal-velocity model with $\beta_0 = 1$ is the most unstable model of type A and B. However if $\beta_0 = 0$, we are dealing with a completely unrealistic model in that it allows for crashes due to the absence of reactions to the next car ahead. The same conclusions hold true for models of type C.

7 Numerical results: discrete multiple look-ahead OV models

Multiple look-ahead and its associated modified linear stability have a profound effect both on the fundamental diagram [20] as well as on travelling wave solutions, especially shock wave solutions of stop-and-go wave patterns. The upstream speed of such waves increases with stronger coupling to further cars ahead, which is what one would expect from intuition. In addition, the hysteresis of stop-and-go traffic, a limit cycle in the phase space of a vehicle as it passes through such traffic, is less pronounced due to increased anticipation of traffic ahead [4]. These observations hold true for models of both types.

7.1 Acceleration, waves and crashes

We now turn to the main problem of the standard OV model, the unrealistic acceleration that arises in the numerical predictions of the vehicle motion.

It turns out that among the three means of trying to restrict these values to more realistic magnitudes, (cut-off, delay and multiple-look ahead), multiple-look ahead proves most useful. For example, taking $\beta_0 = 0.5$, $\beta_1 = 0.3$ and $\beta_2 = 0.2$, the maximum values of acceleration and deceleration at $a = 1.0\ \mathrm{s}^{-1}$ in model A are about $3.8\ \mathrm{m/s}^2$, whereas for model B, we found $4.4\ \mathrm{m/s}^2$. Both values, and in particular model A, are very close to, if not exactly what one finds in real traffic. Figure 2 shows an example of acceleration in a double look-ahead model with $\beta_1 = 0.3$. Moreover, crashes only occur at very low values of the sensitivity, a, or very extreme flow situations.

The dimensionless OV model [1] with

$$V(b) = \tanh(b - 2) + \tanh(2) \tag{21}$$

also shows the large impact of many-neighbour coupling on travelling wave solutions and associated values for the acceleration. In Figure 6, travelling wave solutions are shown for three types of multiple look-ahead, connecting upstream headway, $b_u = 3.0$, with downstream headway, $b_d = 1.8$. The length scale, over which adjustments take place, changes from about $\Delta x = 20$ to $\Delta x = 50$ as the driver increasingly anticipates events further downstream. Correspondingly, the magnitude of the maximum acceleration drops from about 0.5 to 0.1, a very significant change, revealed in Figure 7.

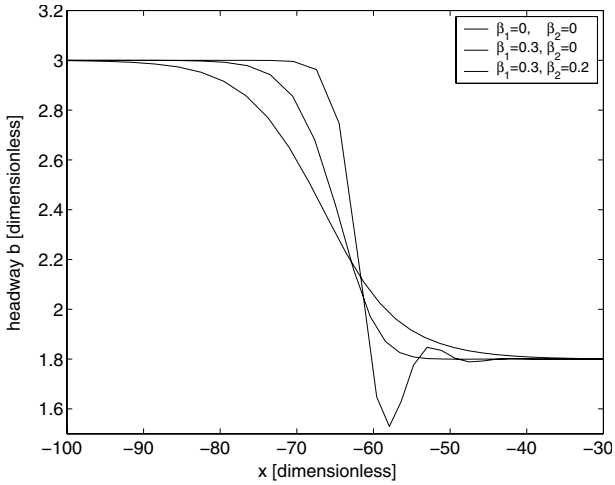

Fig. 6. Travelling wave solutions for three types of multiple look-ahead (single, double and triple) connecting upstream headway, $b_u = 3.0$, with downstream headway, $b_d = 1.8$.

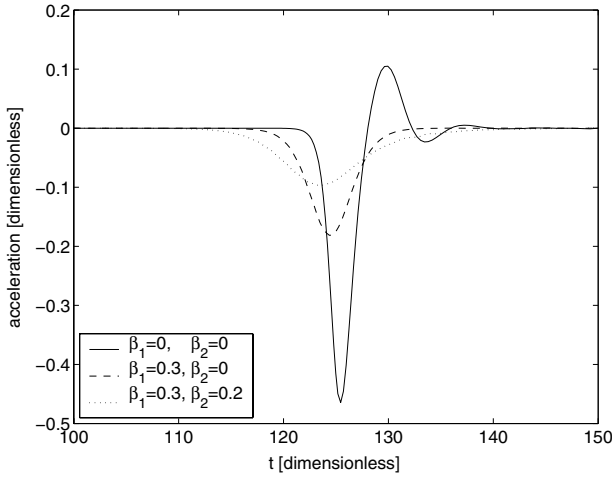

Fig. 7. Acceleration of a vehicle as it moves through the travelling wave profiles of Figure 6.

For the same look-ahead models, Figure 8 exhibits a snapshot of vehicles accelerating almost from rest to almost maximum speed. The shape of the knee that develops again depends on the model, and the slope becomes more gentle with increasing look-ahead. In accordance with the previous findings, the maximum acceleration again decreases significantly, this time by a factor of about 4 (see Fig. 9).

We see that realistic multiple look-ahead parameters significantly reduce the magnitudes of the maximum acceleration inherent in the system and might lead the way to more realistic models. Generally, the values of $\{\beta_i\}$ depend on the traffic situation and would vary with time and space.

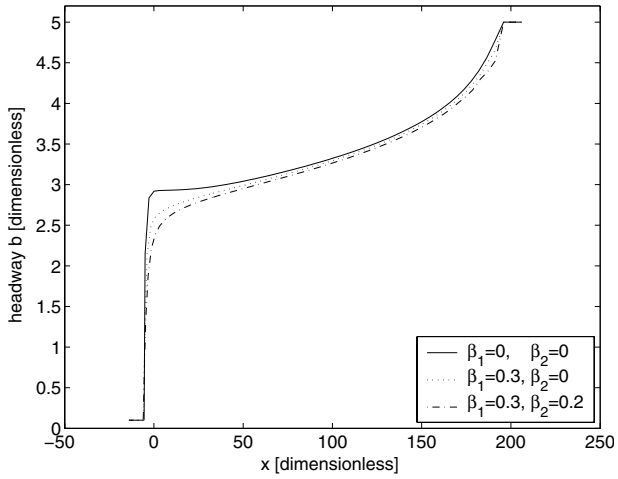

Fig. 8. Wave solutions for three types of multiple look-ahead (single, double and triple) connecting upstream headway, $b_u = 0.1$, with downstream headway, $b_d = 5.0$.

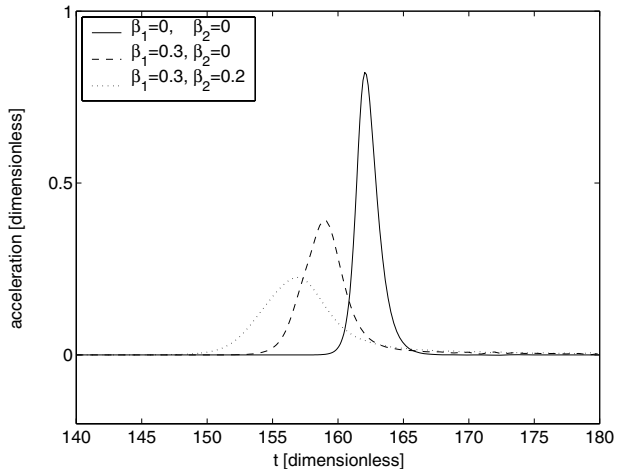

Fig. 9. Acceleration of a vehicle as it moves through the wave profiles of Figure 8.

This leaves the question as to how the parameters β_j $(j = 1, ..., k)$ and the sensitivity a might be determined, once an OV function has been chosen. In order to reproduce realistic traffic flow, we must make the following minimal demands:

1. the fundamental diagram must contain a region of instability over a density regime in accordance with real traffic data;
2. upstream travelling shock waves of stop-and-go traffic must have the right magnitude of speed;
3. maximum values of acceleration and deceleration must be within realistic orders;
4. $\beta_j < \beta_{j+1}$ for $j = 1, 2, 3, ..., k$;
5. it is reasonable to assume a maximum amount of vehicles ahead which have an effect on the driver, e.g. $k = 2$ or $k = 3$;
6. crashes should not occur in simulations of "moderate" flow conditions.

Therefore, we believe that the choice $\beta_0 = 0.5$, $\beta_1 = 0.3$, $\beta_2 = 0.2$ is very reasonable for the OV model as presented in this paper.

However, similar requirements should be made for *any* car-following model that contains multiple look-ahead. Moreover, multiple look-ahead may even prove inevitable in order to fulfil all these requirements. At this point, we should refer to the work of Nagatani [20] who studied the dynamics of the difference equation (9), representing multiple look-ahead (and delay). The author found in accordance with the results of this paper that many-neighbour coupling stabilises the flow and results in less severe shock waves (and hence acceleration). In addition, it reduces the area of coexisting traffic states in the bifurcation diagram. This gives an indication on how strong the effect of multiple look-ahead can be, resulting in non-local continuum models (Sect. 8), and that it needs to be further investigated.

7.2 Synchronised flow

While a detailed investigation of how many-neighbour interaction might be linked to the phenomena of synchronised flow [21,25–28] is beyond the scope of this paper, a brief discussion should highlight where potential modelling advantages of next-to-nearest neighbour models lie.

As speculated by Lenz et al. [4], multiple look-ahead enhances driving in small platoons and might be coupled to the phenomena of synchronised flow [24]. In addition, it seems to be a more realistic model both with respect to real driver anticipation of the flow and the maximum values of acceleration. While the latter is certainly true in dense traffic, the first speculation has not been validated to-date and is questionable since synchronised flow is mainly triggered by inhomogeneities (such as on-ramps) rather than by the vehicle dynamics on a straight road. In fact, only the car-following model as proposed by Kerner and Klenov [21] has been shown to exhibit synchronised flow solutions. However, it differs from "classical" car-following models in a sense that it is based on the assumption of multiple steady states. Moreover, its governing equation is a complex difference equation with a time step size of about 1 second, effectively representing delay. This is similar in spirit to Nagatani's model (9) [20]. While a difference equation, where the step size compares to the reaction time, might be a controversial traffic model, it surely adds realism to the model through the inherent delay.

At this point, it remains unclear as to how to produce a multitude of steady states with a simple car-following model based on differential delay equations and multiple look-ahead alone, without their explicit introduction through a model similar to Kerner and Klenov's. However, Nagatani showed [20] that multiple look-ahead changes the shape of the fundamental diagram. This leads to the question whether dynamic many-neighbour interaction, i.e. $\frac{d}{dt}\beta_i \neq 0$, should enter a realistic microscopic traffic model, especially since the β_i will depend on the traffic

density. This is surely an interesting issue for future research. Another point, which remains unresolved to the authors, is whether the Kerner-Klenov model exhibits realistic values for acceleration and braking. Furthermore, it should also be investigated as to how many-neighbour coupling would change the flow predictions of the Kerner-Klenov model.

8 Non-locality in continuum models

We now focus on the problem of how to incorporate multiple look-ahead into continuum models. This section will explore three such approaches for model A, where a similar analysis applies to model B.

8.1 Approach 1

Car-following models can be linked to a continuum counterpart using a transformation relating the headway b_n of the n-th car, located at x_n, to the local density of the flow, $\rho(x_n, t)$. Berg et al. [29–32] have shown that a natural way of defining such a transformation is by demanding

$$\int_{x_n}^{x_n+b_n} \rho(y,t)\,dy = 1, \tag{22}$$

followed by an extension of x_n to all real numbers describing the road segment. In turn, b_n becomes a continuous function of x, $b(x)$, via

$$\int_{x}^{x+b(x)} \rho(y,t)\,dy = 1. \tag{23}$$

This transformation implies conservation of cars, and preserves the stability criterion (at large wave lengths) and wave solutions [30]. Therefore, it has been regarded as a continuum analogue.

For multiple look-ahead, we can hence define the continuum analogue of model A formally as

$$v_t + vv_x = a\left\{\sum_{j=0}^{k} \beta_j V(b_j(x)) - v\right\}, \tag{24}$$

with local headways, $b_j(x)$, defined iteratively by

$$\int_{x}^{x+b_0} \rho(x+y,t)\,dy = 1, \tag{25}$$

$$\int_{x+\sum_{m=0}^{j-1} b_m}^{x+\sum_{m=0}^{j} b_m} \rho\left(x + \sum_{m=0}^{j-1} b_m + y, t\right) dy = 1 \quad (1 \le j \le k). \tag{26}$$

We observe that multiple look-ahead models are linked to non-local continuum models expressed by partial differential equations coupled to integral equations for the headway. This results in a very complex formulation reminiscent in its simplest form of the non-local continuum model suggested by Nagatani [33,34]

$$(\rho v)_t = \bar{a}\rho_o \bar{V}(\rho(x+1)) - \bar{a}\rho v, \tag{27}$$

which is, like equations (24–26), closed by the conservation of cars

$$\rho_t + (\rho v)_x = 0. \tag{28}$$

However, while Nagatani approximates the various headways, b_j, by an average headway (here: dimensionless headway one), we are now dealing with a complete macroscopic description of the microscopic multiple look-ahead model.

It suffices to say that a numerical simulation of the above continuum model, (24), (25), (26) and (28), poses extreme demands to computational power. However, being an exact analogue of the original multiple look-ahead OV model (8) in the spirit of previous transformations [30], it is a good starting point for further analysis of the continuum description.

8.2 Approach 2

For the standard OV model, Berg et al. [30] showed how to approximate the local headway by the local density using (23) in order to obtain a closed system of partial differential equations (PDE) in density and velocity. The approximation, based on a Taylor expansion of the integral (23), is the more accurate, the more terms are being kept in the expansion. In essence, the non-local effects contained in (22) are approximated by local values, $v(x,t)$ and $\rho(x,t)$, and their derivatives.

When the interaction with additional vehicles ahead is growing, this procedure increasingly fails. This is due to the fact that multiple headways must then be approximated by a small number of local terms in some sort of Taylor expansion (see next Sect. 8.3).

This encourages us to define a non-local continuum model of the form

$$v_t + vv_x = a\left[\int_{-\infty}^{\infty} K(x,y,t)\,V(\rho(x+y)^{-1})\,dy\right] - av \tag{29}$$

with $v = v(x,t)$ and $\rho = \rho(x,t)$, closed by the conservation of cars, equation (28). The kernel K describes the interaction with the vehicles ahead; the dissipative and pressure effects [30] are inherent parts of the model through the integral.

We define the *sphere of influence* s to be the maximum distance ahead, whose traffic events a driver reacts to. Moreover, we might take $K(x,y,t) = K(y)$ on a road of uniform characteristics, and restrict it to monotonicly decreasing functions in y with $K(y) = 0,\ y < 0$. Then, (29) yields

$$v_t + vv_x = a\left[\int_0^s K(y)\,V(\rho^{-1}(x+y))\,dy\right] - av. \tag{30}$$

This equation, closed by conservation of cars in equation (28), forms an integro-differential equation for the density and speed. It contains non-local terms in the integral.

Arguably, the driver behaviour, and hence the dynamics of the flow, are now incorporated in the kernel K. For multi-species traffic consisting of different driver types and/or vehicles [11], the kernel $K(x, y, t)$ has to "flow" with the vehicles

$$K_t + vK_x = 0, \tag{31}$$

where we take the initial distribution to be $K(x, y, 0) = K_0(x, y)$. The description becomes intrinsically more complex at on- or off-ramps as well as for lane-changing manoeuvres on multi-lane highways. A question that arises here is whether a time- and space-dependent K, $K(x, y, t)$, might explain synchronised flow solutions [24].

8.3 Approach 3: k = 1

For double look-ahead ($k = 1$), we now derive a continuum model from equations (24, 25) by approximating the integral equation (25) to second order as in [30]

$$b = \frac{1}{\rho} - \frac{\rho_x}{2\rho^3} - \frac{\rho_{xx}}{6\rho^4} + \frac{\rho_x^2}{2\rho^5}. \tag{32}$$

Moreover, we write formally to first order

$$\begin{aligned} v_t + vv_x &= a\left\{\beta_0 V(b_1) + \beta_1 V(b_2) - v\right\} && (33)\\ &\approx a\left\{\beta_0 V(b_1) + \beta_1 V(b_1 + b_x b_1) - v\right\} && (34)\\ &\approx a\left\{\beta_0 V(b_1) + \beta_1 V(b_1) + \beta_1 V'(b_1)\, b_{1,x} b_1 - v\right\} && (35)\\ &= a\left\{V(b_1) + \beta_1 V'(b_1)\, b_{1,x} b_1 - v\right\}. && (36) \end{aligned}$$

This is the standard model with a first order correction term $\beta_1 V' b_x b$ (dropping the subscript "1"). Substitution for b via equation (32) reproduces the continuum model of the OV model as presented by Berg et al. [30] with a correction term in β_1

$$\begin{aligned} &\rho_t + (v\rho)_x = 0, && (37)\\ &v_t + vv_x = a\left[\hat{V}(\rho) - v\right] \\ &\qquad + a\hat{V}(\rho)\left[(1+2\beta_1)\frac{\rho_x}{2\rho} + \frac{\rho_{xx}}{6\rho^2} - (1+\beta_1)\frac{\rho_x^2}{2\rho^3}\right] && (38) \end{aligned}$$

with $\hat{V}(\rho) = V(1/\rho)$. Hence, we expect this to be a reasonable approximation only for $\beta_1 \ll 0.5$. We see that the effect of multiple look-ahead shows in the modification of the pressure and nonlinear pressure term, with corrections to the diffusive term expected at higher orders.

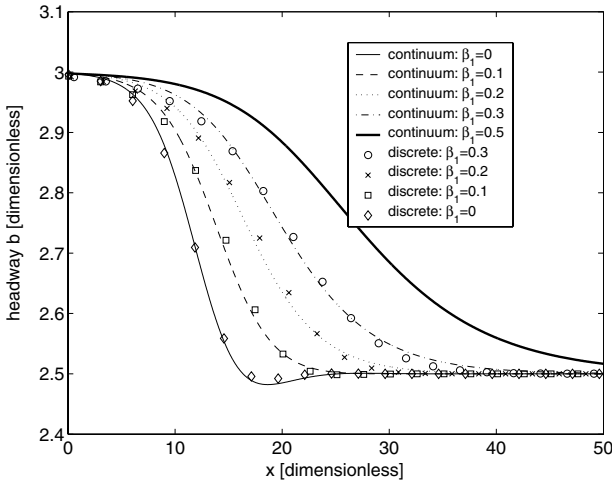

Fig. 10. Comparison of travelling wave solutions for double look-ahead in the dimensionless OV model: discrete and continuum models. Moderate transition from $b_u = 3.0$ to $b_d = 2.5$. Note that the case $\beta_1 = 0.5$ leads to crashes in the discrete model, whereas the continuum model predicts a (unstable) travelling wave.

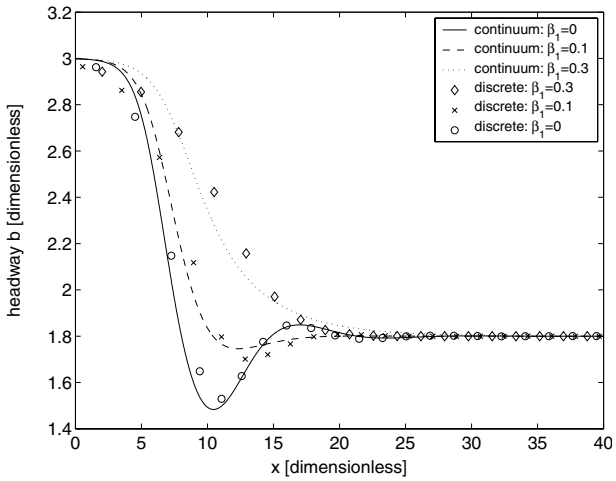

Fig. 11. Comparison of travelling wave solutions for double look-ahead in the dimensionless OV model: discrete and continuum models. Transition from $b_u = 3.0$ to $b_d = 1.8$.

9 Travelling waves in discrete and continuum multiple look-ahead OV models

As expected, the third approach works the better, the less significant the look-ahead is. With increasing anticipation of (nonlocal) events further downstream, the (local) Taylor expansion is less accurate as illustrated in Figures 10 and 11. Nevertheless, the length scales over which adjustments take place, are predicted rather accurately by the continuum model, even in the case of $\beta_1 = 0.3$. The profiles of the discrete model and the corresponding continuum model resemble each other with less accuracy, though. This trend is more pronounced, the larger the drop in headway across the wave is, and the larger the look-ahead parameter β_1 is. Note that our travelling wave

analysis in the continuum model does not discuss stability of such waves. Hence, the (unstable) travelling wave solution as predicted by the continuum model at $\beta_1 = 0.5$ (Fig. 10) is never observed in the initial value solver of the discrete OV model. Instead, such a drop in headway leads to crashes.

This is one indication that this method will increasingly fail with higher order look-ahead such as in Figures 6 and 8. Therefore, it has its limits but shows that multiple look-ahead might have been included in continuum models such as the Kerner-Konhaeuser model [35] through the fitting of the pressure and diffusion coefficients to traffic data, which naturally includes many-neighbour interaction.

10 Discussion

An analysis of the standard optimal-velocity model [1,2], including a dimensional optimal-velocity (OV) function, reveals unrealistic values for the acceleration and breaking. We suggested four ways of dealing with this problem: modifying the OV function, limiting acceleration and breaking by cut-offs, introducing time delay, and including multiple look-ahead.

We found that only the latter approach is a promising candidate to lead to models which fulfil the following requirements at the same time: (1) the fundamental diagram must contain a region of instability over a density regime in accordance with real traffic data, (2) the speed of stop-and-go shock waves must have the right order of magnitude, (3) the maximum values of acceleration and deceleration must be within realistic orders, and (4) crashes should not occur in the simulations of moderate flow conditions. These requirements should be posed for all car-following models. Recent model validations [15] might reveal as to how far this can be reproduced by various models.

We believe that multiple look-ahead should not only be included in the optimal-velocity model, but it might also have a significant impact on flow simulations, especially when combined with delay or random effects [36] such as multi-species flow [11]. Whether many-neighbour interaction is a necessary modelling tool to reproduce synchronised flow [4,24] remains an unsolved issue, but it poses a number of questions for future work, e.g. how multiple look-ahead affects meta-stability [37]. What can be concluded is that multiple look-ahead results in a stabilisation of uniform flow solutions.

P. B. would like to thank Boris Kerner for his discussions about and clarifications of the phenomena of synchronised flow, three-phase traffic and the universal features of certain traffic flow models.

Appendix A: Stability analysis

This appendix briefly derives the stability criteria for model A.

Recall that $\dot{b}_n = v_{n-1} - v_n$ and $\ddot{b}_n = \dot{v}_{n-1} - \dot{v}_n$, so that subtracting the governing equations of two adjacent vehicles using (8) gives

$$\frac{\ddot{b}_n}{a} + \dot{b}_n - \sum_{j=0}^{k} \beta_j \left[V(b_{n-j-1}) - V(b_{n-j})\right] = 0. \qquad (39)$$

As usual, we perturb around the uniform flow solution $b_n = b$ by small amounts $\tilde{b}_n$ and then linearise to find

$$\frac{\dddot{\tilde{b}}_n}{a} + \dot{\tilde{b}}_n - V'(b) \sum_{j=0}^{k} \beta_j \left[\tilde{b}_{n-j-1} - \tilde{b}_{n-j}\right] = 0. \qquad (40)$$

It is appropriate to look for solutions of the form $e^{\lambda t} e^{in\xi}$, where $\xi = 2\pi m/N$, $m = 0, \ldots, N-1$, and N the number of vehicles on a circular road [2]. This gives the characteristic equation

$$\frac{\lambda^2}{a} + \lambda - V'(b) \sum_{j=0}^{k} \beta_j \left[e^{-i(j+1)\xi} - e^{-ij\xi}\right] = 0. \qquad (41)$$

This is a quadratic equation for λ, which can in principle be solved explicitly. However, it is more instructive to identify parameters at the onset of instability (neutral stability) by setting $\lambda = i\omega$ for some real ω to give

$$-\frac{\omega^2}{a} + i\omega - V'(b) \sum_{j=0}^{k} \beta_j \left[e^{-i(j+1)\xi} - e^{-ij\xi}\right] = 0, \qquad (42)$$

which splits into real and imaginary parts,

$$\text{Re: } 0 = -\frac{\omega^2}{a} - V'(b) \sum_{j=0}^{k} \beta_j \left\{\cos[(j+1)\xi] - \cos(j\xi)\right\}, \qquad (43)$$

$$\text{Im: } 0 = \omega + V'(b) \sum_{j=0}^{k} \beta_j \left\{\sin[(j+1)\xi] - \sin(j\xi)\right\}. \qquad (44)$$

We eliminate ω to find a relationship involving only $V'(b)$, ξ and a,

$$\frac{V'(b)}{a} = -\frac{\sum_{j=0}^{k} \beta_j \left\{\cos[(j+1)\xi] - \cos(j\xi)\right\}}{\left\{\sum_{j=0}^{k} \beta_j \left\{\sin[(j+1)\xi] - \sin(j\xi)\right\}\right\}^2}. \qquad (45)$$

A.0.1 All β_i equal

Let us take the assumption that $\beta_j = \beta = 1/(k+1)$ for all j. Then equation (45) can be simplified to

$$\frac{V'(b)}{a} = -\frac{\left\{\cos[(k+1)\xi] - 1\right\}(k+1)}{\sin^2[(k+1)\xi]}. \qquad (46)$$

The right hand side of this equation potentially has singularities where the denominator vanishes, i.e. at

$\xi = 0, \pi/(k+1), 2\pi/(k+1), \ldots, k\pi/(k+1), \pi$. (We consider only $\xi \in [0, \pi]$, because of the even symmetry in this formula.)

For $\xi = 0, 2\pi/(k+1), 4\pi/(k+1)$, etc., the numerator also vanishes. Thus it is necessary to use L'Hôpital's rule to find the value of the right hand side at these points. Differentiating the top and bottom of the right hand side of equation (46) with respect to ξ gives

$$\frac{(k+1)^2 \sin[(k+1)\xi]}{2(k+1)\sin[(k+1)\xi]\cos[(k+1)\xi]} = \frac{k+1}{2\cos[(k+1)\xi]}. \tag{47}$$

So by L'Hôpital, the right hand side of equation (46) tends to $(k+1)/2$ as $\xi \to 2l\pi/(k+1)$, where $l = 0, 1, \ldots$

For $\xi = \pi/(k+1), 3\pi/(k+1), 5\pi/(k+1)$, etc., the numerator of equation (46) is nonzero while the denominator is zero, leading to the limit of the right hand side of equation (46) being infinity as $\xi \to (2l-1)\pi/(k+1)$, where $l = 1, 2, \ldots$

A.0.2 The $\xi = 0$ mode

The fact that we have found the global minimum of the right hand side of equation (45) in all cases (Figs. 3–5) at $\xi = 0$, leads us to suspect that this holds for all possible vectors $\boldsymbol{\beta}$. Due to symmetry reasons, we know that we always have a local extremum at $\xi = 0$. Without explicit proof, however, we assume that this coincides with the global minimum and derive the global stability criterion for this scenario.

We want to determine the limit of the right hand side of equation (45) as $\xi \to 0$. Applying L'Hôpital's rule once and using the series expansions of $\cos(x)$ and $\sin(x)$ about $x = 0$, we obtain the neutral stability criterion

$$\frac{V'(b)}{a} = \frac{1}{2}\sum_{j=0}^{k} \beta_j (2j+1). \tag{48}$$

The standard OV model is retrieved at $k = 0$.

References

1. M. Bando, K. Hasebe, K. Nakanishi, A. Nakayama, A. Shibata, J. Phys. I France **5**, 1389 (1995)
2. M. Bando, K. Hasebe, A. Nakayama, Y. Sugiyama, Phys. Rev. E **51**, 1035 (1995)
3. S. Hooper, *Modifications of Bando's car-following model of highway traffic*, MSc thesis, University of Bristol, UK (2000)
4. H. Lenz, C.K. Wagner, R. Sollacher, Eur. Phys. J. B **7**, 331 (1999)
5. D. Helbing, Rev. Mod. Phys. **73**, 1067 (2001)
6. D. Chowdhury, L. Santen, A. Schadschneider, Phys. Rep. **329**, 199 (2000)
7. T. Nagatani, Rep. Prog. Phys. **65**, 1331 (2002)
8. K. Nakanishi, K. Itoh, Y. Igarashi, M. Bando, Phys. Rev. E **55**, 6519 (1997)
9. M. Bando, K. Hasebe, K. Nakanishi, A. Nakayama, Phys. Rev E **58**, 5429 (1998)
10. H. Hayakawa, K. Nakanishi, Phys. Rev. E **57**, 3839 (1998)
11. E.N. Holland, A.W. Woods, Trans. Res. B **31**, 473 (1997)
12. A.D. Mason, A.W. Woods, Phys. Rev. E **55**, 2203 (1997)
13. P.G. Gipps, Trans. Res. B **15**, 105 (1981)
14. Y. Sugiyama, Presentation at *Traffic and Granular Flow'03*, 02/10/2003, TU Delft, Netherlands
15. P. Wagner, I. Lubashevsky, *Traffic and Granular Flow'03* (Springer, 2004), submitted
16. N.F. Abou-Rahme, Transfer dissertation (1999)
17. L.C. Davis, Phys. Rev. E **66**, 038101 (2002)
18. M. Green, Transp. Hum. Factors **2**, 195 (2000)
19. T. Nagatani, K. Nakanishi, Phys. Rev. E **57**, 6415 (1998)
20. T. Nagatani, Phys. Rev. E **60**, 6395 (1999)
21. B.S. Kerner, S.L. Klenov, J. Phys. A **35**, L31 (2002)
22. C. Wagner, Physica A **260**, 218 (1998)
23. Y. Sugiyama, H. Yamada, *Traffic and Granular Flow'97* (Springer, 1998), pp. 301–318
24. B.S. Kerner, Trans. Res. Rec. **1678**, 160 (1999)
25. B.S. Kerner, Physica A **333**, 379 (2004)
26. B.S. Kerner, S.L. Klenov, Phys. Rev. E **68**, 036130-1 (2003)
27. B.S. Kerner, S.L. Klenov, D.E. Wolf, J. Phys. A **35**, 9971 (2002)
28. B.S. Kerner, Phys. Rev. E **65**, 046138-1 (2002)
29. P. Berg, *Optimal-velocity models of motorway traffic*, Ph.D. thesis, University of Bristol, UK (2001)
30. P. Berg, A. Mason, A.W. Woods, Phys. Rev. E **61**, 1056 (2000)
31. P. Berg, A.W. Woods, Phys. Rev. E **63**, 036107 (2001)
32. P. Berg, A.W. Woods, Phys. Rev. E **64**, 035602 (2001)
33. T. Nagatani, Physica A **261**, 599 (1998)
34. T. Nagatani, Physica A **264**, 581 (1999)
35. B.S. Kerner, P. Konhäuser, Phys. Rev. E **50**, 54 (1994)
36. R. Mahnke, J. Kaupuzs, Phys. Rev. E **59**, 117 (1999)
37. P. Berg, R.E. Wilson, *Traffic and Granular Flow'03* (Springer, 2004), submitted